

Advanced statistical analysis of Local Bubble Size Distributions in 2D gas fluidized beds

Antonio Busciglio¹, Giorgio Micale¹, Lucio Rizzuti¹, Giuseppa Vella¹,
Alberto Lombardo²

¹Dipartimento di Ingegneria Chimica dei Processi e dei Materiali

²Dipartimento di Tecnologia Meccanica, Produzione ed Ingegneria Gestionale
Università degli Studi di Palermo, Viale delle Scienze ed. 6, 90128, Palermo Italy

The principal difficulty in analysing fluidization quality and bubble dynamics is related to the possibility of measuring or predicting the physical and geometrical properties of gas bubbles rising in a granular medium. Even the development of detailed experimental correlations gives poor results, being necessary a fully statistical approach. On the above basis, the present work focuses on the statistical analysis of the behaviour of a 2-D fluidized bed operating under bubbling and slugging conditions, performing measurements of Local Bubble Size Distributions (BSD) along the bed. The analysis allowed to observe a characteristic bimodal shape of BSDs for different particles dimension and fluidization velocities, due to the contemporary presence of random coalescence, splitting and nucleation phenomena. The presence of a characteristic peak of the distribution at small diameters accounts for the enhanced mixing effects due to small bubbles, while the second peak is related to large bubbles responsible for gas by-pass. Conversely, an almost Gaussian distribution is obtained when a BSD weighed on bubble area is computed.

1. Introduction

Several studies can be found in literature regarding the bubble diameter evolution along their path along the bed due to coalescence/splitting phenomena (Darton et al. [1977], Agarwal [1985], Mori and Wen [1975], Horio and Nonaka [1987], Shen et al. [2004]). These studies well indicate how bubble diameter evolution influences bubble rise velocities, reaction kinetics and mass transfer coefficients. The phenomenon of bubble evolution starts with the nucleation in the region immediately above the distributor. The rise of bubbles along bed height shows a chaotic behaviour, the rise path being affected by lateral random fluctuations, lateral capture by wake regions of other bubbles, shearing-off of small bubbles from larger ones, bubble ruptures due to surface instabilities, random nucleation of new bubbles in the emulsion phase. All these behaviours are extremely difficult to be modelled, and they make simple correlations inadequate to describe bubble dynamics. A useful approach to tackle the problem involves the measurement of Bubble Size Distribution (BSD) along the bed, in order to statistically characterize the bubbles behaviour. In the work by Park et al. [1969], the BSDs in gas fluidized beds are computed. The mean of BSD increases with i) elevation above the distributor, ii) inlet gas velocity and iii) particle diameter. Moreover, the authors underline that the measured distributions appear to gradually become positively

skewed when the probe is placed at increasing distances above the distributor. On these grounds, Werter [1974] and Van Lare et al., [1997], adopted a log-normal distribution in order to fit experimentally measured BDS. While several other studies (Argyriou et al. [1971], Morooka et al. [1972], Rowe and Yacono [1975], Liu and Clark [1995]) adopted Gamma distributions in order to fit BSD data: in fact, the Gamma distribution can be theoretically justified on the basis of the coalescence phenomena, as demonstrated by Argyriou et al. [1971].

In the present work, the experimentally measured BSD in 2D gas-fluidized beds via Digital Image Analysis Technique (Busciglio et al. [2008]) have been fitted with an original combination of distribution functions, in order to highlight the coalescence and splitting phenomena that characterize bubbling fluidized beds. Full details on measurement techniques and devices, and experimental set up can be found in the work of Busciglio et al. [2008].

2. Experimental set-up

The fluid-bed reactor purposely designed and built for the present investigation is made of Perspex® with dimensions equal to 800 (height) x 180 (width) x 15 (depth) mm. Air was used as fluidizing gas, whose flow rate was accurately measured through a set of four flow-meters, covering the range 0-140 lt/min. Two kind of particulates were used for the experimental runs, in particular glass ballotini with density equal to 2500 kg/m³ having size ranges of 212-250 µm (fluidized at inlet gas velocities equal to 1.7, 3.4, 5.0 and 7.0 times the u_{mf}) and 500-600 µm (fluidized at inlet gas velocities equal to 1.2, 1.4 and 1.7 times the u_{mf}). The particles were filled up to a bed height of 360 mm, i.e. twice the bed width. The bubble-related flow structures were visualized with the aid of a back-lighting device and recorded by a digital camcorder (mvBlueFox 121c).

The image processing routine was developed on Matlab 7.3 (The MathWorks inc.), using the Image Processing Toolbox. Full reference about the image acquisition and elaboration procedure (DIAT) can be found in Busciglio et al. [2008].

For each experiment, the local non-parametric Bubble Size Distributions (BSD) weighed on bubble number and bubble projected area have been computed. Four Region Of Interest (ROI) have been selected from the entire field of view: in particular regions having the same width of the fluid bed and height of 5 cm have been chosen. The ROI centres are located at four different elevations above the distributor, i.e. 0.25, 0.50, 0.75 and 1.00 H_0 , where H_0 is the settled bed height at rest.

3. Discussion and result

In Fig. 1, the experimental distribution of bubble equivalent diameters is reported as function of bubble distance from distributor for two of the investigated cases, in particular the experiment with 212-250 µm particulate fluidized at 3.4 and 5.0 u_{mf} respectively. The cloudy data presented allow the visualization of the small bubbles that are inside the bed even at the highest elevations. On the whole the experimental data show a characteristic increase in bubble diameter, with an upper envelope of data approximately following a power law, in accordance with the analysis by Darton et al.

[1977]. However, the presence of a wide distribution of bubble sizes is evident at all elevations of the bed, as a result of the splitting and/or nucleation phenomena.

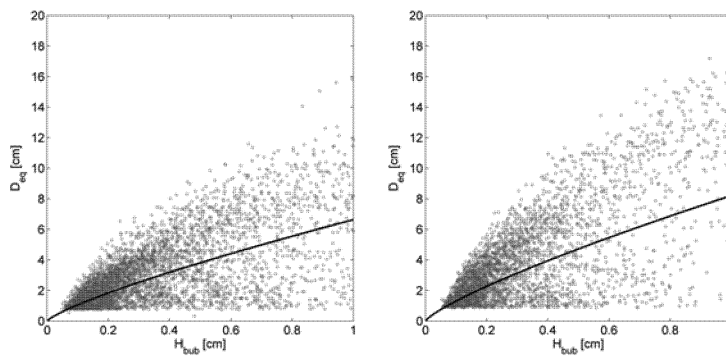


Figure 1. Raw data for 212-250 μm particulate fluidized at $3.4 u_{mf}$ (left) and $5.0 u_{mf}$ (right).

The analysis of bubble size distributions computed in regions at different elevations above the distributor for the case of 212-250 μm particles fluidized at $3.4 u_{mf}$ shows a characteristic bimodality of BSD, as can be seen in Fig. 2 (left). The different shapes of local BSD at different elevations can be ascribed to the coalescence and break-up phenomena occurring in the fluidized bed. In fact, at each elevation analyzed, with the exception of the measurements taken at $0.25H_0$, it is possible to find a fraction of bubbles having considerably smaller size than that expected at that particular elevation, whose genesis is related to nucleation and break-up phenomena occurring at that elevation. Conversely the complementary fraction of bubbles having the expected size for that elevation naturally originates from coalescence and growth of bubbles from inferior regions of the bed.

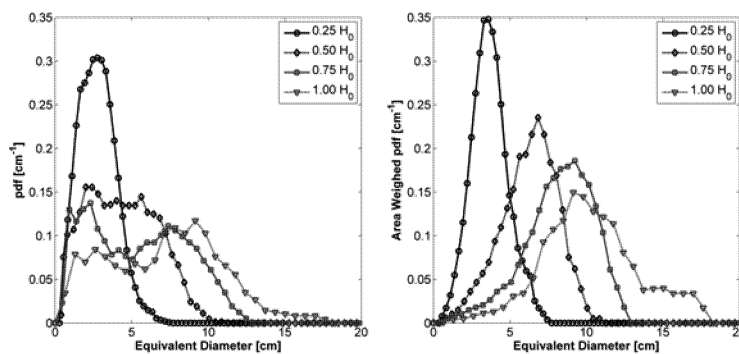


Figure 2. BSD (left) and area weighed BSD (right).

This mechanism is able to describe the bimodal pattern of BSD in fluidized beds: the primary peak (i.e. smaller bubble sizes) is due to local nucleation and splitting phenomena, and thus its mean and mode value does not change with elevation above the distributor. Conversely, the secondary peak (i.e. larger bubble sizes) will increase its

mean and mode value with the elevation, as physically expected because of the above-mentioned coalescence phenomena.

The bimodal pattern of local BSD is a substantially new finding with respect of the previous works regarding fluidized beds BSD. Such evidence can be properly quantified by means of a fitting function, resulting by the sum of two gamma distribution functions:

$$BSD_{gamma} = \varphi \frac{x^{\alpha_1-1}}{\beta_1^{\alpha_1} \Gamma(\alpha_1)} e^{-\frac{x}{\beta_1}} + (1-\varphi) \frac{x^{\alpha_2-1}}{\beta_2^{\alpha_2} \Gamma(\alpha_2)} e^{-\frac{x}{\beta_2}} \quad (1)$$

Where the first distribution is relevant to the small diameter peak (primary peak) and the second is relevant to larger diameter peak (secondary peak or moving peak).

Conversely, the analysis of area weighed BSD, reported in figure 2 (right) shows a characteristic unimodal distribution whose mean and mode values increase with elevation above the distributor, and can be adopted to characterize the bubble related gas by-pass. The small skewness of such distribution suggest the use of simple normal distribution as proper fitting function:

$$BSD_{normal} = \frac{1}{\sigma_B \sqrt{2\pi}} e^{-\frac{(x-\mu_B)^2}{2\sigma_B^2}} \quad (2)$$

For each region of interest the following quantities can be thus computed: i) mean value of the sample (D_{10}); ii) area weighed mean value (D_{21}); iii) mean value of the area weighed BSD fitting function and relevant standard deviation (μ_B , σ_B); iv) mean, mode, standard deviation and skewness for each of the components of the gamma BSD (μ_1 , μ_2 , mode₁, mode₂, σ_1 , σ_2 , skewness₁, skewness₂); v) small peak fraction (ϕ).

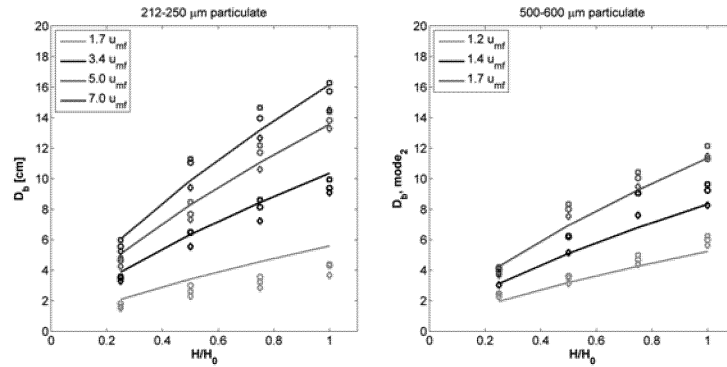


Figure 3. Comparison between experimental data and fitting equation.

The comparison of the measured D_{21} and μ_B as function of the relevant μ_2 highlights that such quantities are practically equal (in the range $\pm 20\%$, without any particular data trend), i.e. thus confirming that the bubbles of the secondary peak are those responsible

of the gas by-pass, being associated with the majority of the bubble areas (μ_B and D_{21}). Moreover, the similar value of mode_2 and μ_2 highlights that the secondary peaks are generally almost symmetrical (low skewness). On these basis, the D_{21} , μ_2 , and μ_B values have been fitted with a Darton-like fitting function (Eq. 3), giving rise to the fitting coefficients reported in the Table 1, together with relevant coefficients as found by Darton et al. [1977] and Shen et al. [2004].

$$d_b = a(u - u_{mf})^\alpha h^\beta \quad (3)$$

	a	α	β
This work	0.225	0.51	0.71
Darton et al. (1977)	0.136	0.40	0.80
Shen et al. (2004)	0.092	0.667	0.667

Table 1. Fitting parameters.

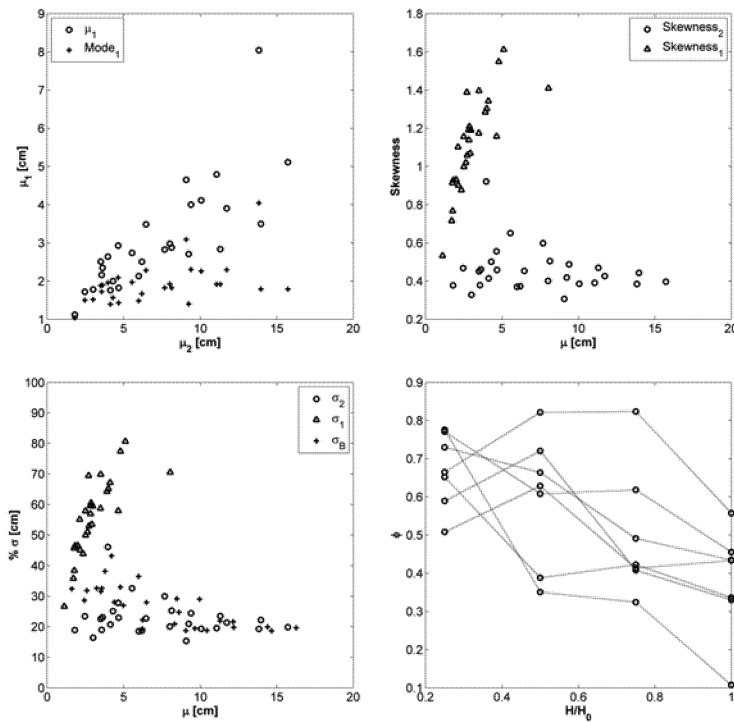


Figure 4. a) μ_1 values as function of relevant μ_2 values; b) gamma distribution skewness; c) percentage standard deviations; d) small diameter fraction (ϕ) values.

It is worth noting that the proposed equation well fits experimental data, with larger errors in the range $\pm 20\%$, as can be seen in figure 3.

Further analyses can be performed on the basis of the measured statistical parameters of the fitting functions adopted to describe both BSD and area-weighted BSD, as reported in Fig. 4. It is possible to observe that the comparison between mean and mode values

of the primary peak, reported as function of the relevant mean value of the secondary peak (Fig. 4.a) highlights an increasing skewness of the primary peak distribution (see also Fig. 4.b). Moreover, it is possible to see that the mode value of the primary peak remains practically unchanged in all cases investigated. The skewness of the primary peak notably changes when the mean value of the secondary peak increases, while that of the secondary peak appear not to change appreciably with operating conditions. Such findings are confirmed by the analysis of the standard deviation as a function of relevant mean values, as reported in Fig 4.c: in fact, the percentage standard deviation varies well for the primary peak, while remains practically unchanged for both secondary peak evolution and area-weighted BSD. As physically expected, the fraction of small bubbles (the ϕ parameter reported in Fig. 4.d) systematically decreases with increasing elevation above the distributor.

4. Conclusions

In this work, a full statistical analysis of bubble size distribution in 2D gas fluidized beds has been performed. The analysis of local Bubble Size Distributions here reported highlighted a bimodality that can be explained through the coalescence/splitting behaviour of bubbles inside the bed, under the hypothesis of separable effects. Such hypothesis has been confirmed, and a correlation for the prediction of secondary peak average diameters has been developed. Moreover, the percentage standard deviation for secondary peak does not changes appreciably with operating conditions. The full statistical characterization of bubbling behaviour can be adopted for more reliable reactor scale-up and design.

Acknowledgements

This work was funded by the Italian Ministry of University within the framework of the PRIN 2005 "Study of fluidized beds stabilized by means of electric or magnetic fields".

References

- Agarwal P.K. (1985), *Chem. Eng. Res. Des.*, 63:323-337.
 Argyriou D.T., List H.L. and Shinnar R. (1971), *AIChE J.* 17:122-130.
 Busciglio A., Vella G., Micale G., Rizzuti L. (2008), *Chem. Eng. J.*, 140:398-413.
 Darton R.C., LaNauze R.D., Davidson J.F., Harrison, D., (1977), *Trans. Instn. Chem. Engrs.*, 55:274-280-
 Horio M. and Nonaka A. (1987), *AIChE J.*, 33:1865-1872.
 Liu W. and Clark N.N. (1995), *Int. J. Multiphase Flow*, 21:1073-1089.
 Mori S. and Wen C.Y. (1975), *AIChE J.* 21:109-115.
 Morooka S., Tajima K., Miyauchi T. (1972), *Int. Chem. Eng.*, 12:168-174.
 Park W.H., Kang W.K., Capes C.E. and Osberg G.L. (1969), *Chem. Eng. Sci.*, 24:851.
 Rowe P. N. and Yacono C. (1975), *Trans. Instn. Chem. Engrs.*, 53:59-60.
 Shen L., Johnsson F., Leckner B. (2004), *Chem. Eng. Sci.*, 52:2607-2617.
 Van Lare C.E.J., Piepers H.W., Schoonderbeek J.N. and Thoenes D. (1997), *Chem. Eng. Sci.*, 52:829-841.
 Werter J. (1974), *Trans. Instn. Chem. Engrs.*, 52:149-159.